O_2-Adduct Complex of *meso*-Tetrakis($\alpha,\alpha,\alpha,\alpha$-*o*-pivalamidophenyl)porphinatoiron(II) with an Intramolecularly Coordinated Proximal Histidine

Teruyuki Komatsu, Yasuko Matsukawa, Kaoru Miyatake, and Eishun Tsuchida*#
Department of Polymer Chemistry, Advanced Research Institute for Science and Engineering, Waseda University, Tokyo 169-8555

(Received April 17, 2001; CL-010350)

meso-Tetrakis($\alpha,\alpha,\alpha,\alpha$-*o*-pivalamidophenyl)porphinatoiron(II) with an intramolecularly coordinated proximal histidine forms a stable O_2-adduct complex in benzene solution at 25 °C; the O_2-binding affinity ($P_{1/2}$: 1.7 Torr) is significantly low compared to that of the *N*-alkylimidazole bound analogue.

Synthetic hemes bearing a covalently bound nitrogenous base have been extensively used for the study of the O_2-, CO-, and NO-binding properties of hemoglobin (Hb) and myoglobin (Mb) over the past few decades.[1–4] The *trans*-coordinated axial base plays a crucial role in the stable O_2-adduct formation and the increase in the O_2-binding constant. However, most of these model compounds have been equipped with an *N*-alkylimidazole or pyridine derivative. Strictly speaking, they are different from nature, where a protoheme binds only to a histidine (F8His) residue in the native Hb. To the best of our knowledge, there are a few reports on the synthetic porphines having a histidine side-chain, but their O_2-binding equilibria and kinetics have never been studied.[5–7] Therefore it is still of great interest to elucidate the dioxygenation behavior of the synthetic heme bearing a proximal histidine. We have recently found that *meso*-tetrakis($\alpha,\alpha,\alpha,\alpha$-*o*-pivalamidophenyl)porphinatoiron(II) or *meso*-tetrakis($\alpha,\alpha,\alpha,\alpha$-*o*-1'-methylcyclohexylamidophenyl)porphinatoiron(II) with an intramolecularly coordinated L-histidine methylester (L-HisOMe) residue forms a stable and reversible O_2-adduct complex in organic solvent at 25 °C. This paper reports for the first time the O_2-binding abilities of these new prosthetic group models for the active sites of Hb and Mb.

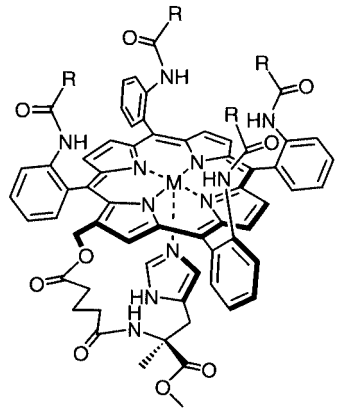

The parent porphines, namely 2-hydroxymethyl-5,10,15,20-tetrakis($\alpha,\alpha,\alpha,\alpha$-*o*-pivalamidophenyl)porphine, was prepared via the Vilsmeir reaction according to our previously reported procedure.[8] The hydroxy group has been converted into a carboxylic acid chain by gulutaric anhydride. An attempt to introduce L-HisOMe into this carboxylic acid by a one-pot reaction using DCC unfortunately failed. Several unknown products were detected. In contrast, the same coupling using benzotriazol-1-yloxytris(dimethylamino)phosphonium hexafluorophosphate in a dry DMF solution yielded the target free-base compound (**1a**) in high yield (>85%). The reaction proceeds smoothly at room temperature, and only washing with water purified the compounds without column chromatography. The 1-methylcyclohexylamido-substituted derivative (**2a**) was also prepared with 1-methylcyclohexanecarboxylic acid. Iron insertion was carried out using $FeBr_2$ in dry THF, affording **1b** or **2b**, which is now available in gram quantities. The analytical data of all compounds described here were satisfactorily obtained.[9]

1b was reduced to the corresponding iron(II) complex (**1c**) by reduction in a heterogeneous two-phase system (benzene/aq. $Na_2S_2O_4$) under an N_2 atmosphere.[8] The UV–vis absorption spectrum of the orange solution of **1c** showed five-*N*-coordinated iron(II) species (λ_{max}: 441, 544, 564 nm, Figure 1), which was constant in the range from 10 μM–3 mM at 10–70 °C. Resonance Raman (RR) spectroscopy showed a medium band at 219 cm^{-1}, which was assigned to the Fe(II)–N(imidazole)

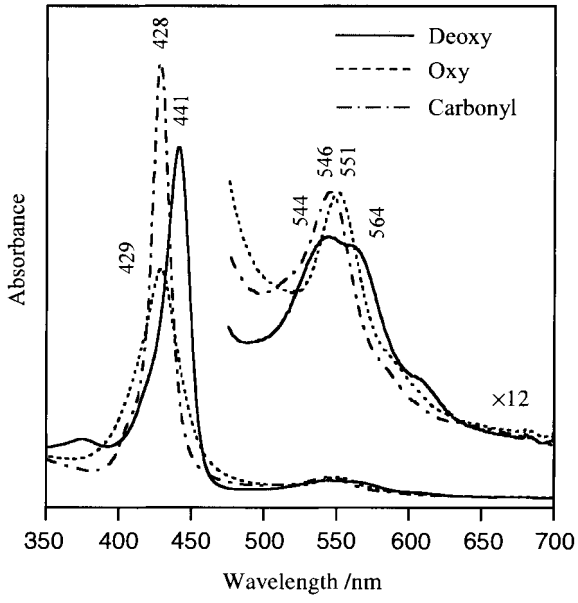

Figure 1. Visible absorption spectral changes of **1c** in benzene at 25 °C.

stretching mode, ν(Fe–N_ε).[10,11] The covalently bound histidine residue at the porphyrin periphery definitely binds to the central iron(II) to give a five-coordinated high-spin iron(II) complex under an N_2 atmosphere.

Upon exposure to O_2 or CO in this benzene solution of **1c**, the UV–vis absorption spectrum immediately changed to those of the O_2 or CO adduct (Figure 1). The dioxygenation was sufficiently stable and reversible at 25 °C depending on the O_2-partial pressure. In the RR spectrum, a new ν(Fe–O_2) vibration of the dioxygenated **1c** appeared at 592 cm^{-1} after O_2 bubbling. This frequency suggests a typical end-on type O_2 coordination to the porphyrinatoiron(II). The skeletal modes of the porphine ring (ν_8 and ν_4) were also upshifted from 370 and 1348 cm^{-1} to 394 and 1366 cm^{-1}, respectively. These observations indicate the conversion of the five-coordinated high-spin iron(II) complex to the six-coordinated low-spin iron(II) complex of **1c**.[10–12] All the observed shifts were reversibly dependent on the O_2 concentration. The 1-methylcyclohexanamido-substituted **2c** also showed the same results. Thus we concluded that **1c** and **2c** having a histidine residue can bind and release the O_2 molecule at ambient temperature. The half-life of the O_2 adducts of **1c** and **2c** were ca. 13 h and 11 h at 25 °C, respectively.

Then the optimum structure of the dioxygenated **1c** complex was simulated.[13] The dihedral angle of the imidazole ring with respect to the porphyrin plane was 89.3°, indicating that the imidazole *N*-coordination to the central iron(II) is not hindered by the rigid spacer between the porphine and HisOMe. It is also remarkable that the H atom of the imidazole ring cannot form a hydrogen bond with the neighboring carbonyl O, which is known to partially influence the dioxygenation of the heme.

The O_2-binding affinity of **1c** ($P_{1/2}$: 1.7 Torr) determined by the UV–vis absorption spectral changes was significantly low compared to that of the *N*-alkylimidazole coordinated analogue, 2-imidazolyloctanoyloxymethyl-5,10,15,20-*tetrakis*($\alpha,\alpha,\alpha,\alpha$-*o*-pivalamidophenyl)porphinatoiron(II) (FeTpivPIm, $P_{1/2}$: 0.29 Torr) (Table 1).[8] Laser-flash photolysis gave the association and dissociation rate constants (k_{on}, k_{off}) of these gaseous ligands.[8,14,15] Kinetically, the high k_{off} of **1c** leads to the low binding affinity of O_2. Since there is no strain in the geometry of the axial base coordination, the small O_2-binding affinity is probably caused by the low σ-basicity of the histidine (pK_a: 6.0). Interestingly, the O_2-binding parameters of **1c** and **2c** became identical. Based on the important earlier studies, the distal steric encumbrance only reduces the association rate for O_2.[1,14,15] Therefore, it is concluded that the inner volume of the cavities, which are constructed by the pivalamido groups and 1-methylcyclohexanamido groups on the porphine macrocycle, are nearly the same.

Table 1. O_2-binding parameters of **1c** and **2c** complexes at 25 °C

	$P_{1/2}$ /Torr[a]	$10^{-8}\,k_{on}$ /$M^{-1}s^{-1}$	$10^{-3}\,k_{off}$ /s^{-1}
1c[b]	1.7	2.1	3.7
2c[c]	1.7	2.0	4.3
FeTpivPIm[c,d]	0.29	3.4	1.4

[a]1 Torr = 133.322 Pa. [b]In benzene. [c]In toluene. [d] ref 8.

These results are the first examples of the stable O_2-adduct complexes of the synthetic porphinatoiron(II)s with an intramolecularly coordinated proximal histidine, and their O_2-binding equilibrium and kinetic parameters. We concluded that covalently attaching the histidine amino acid directly to the porphine side-chain provides the five-*N*-coordinated high-spin iron(II) complex and a relatively small equilibrium constant for the O_2 binding in comparison to that of the *N*-alkylimidazole bound analogue due to the high dissociation rate. The moderately low O_2-binding affinity is significant for design of the O_2-carrier model, because it should release the coordinated O_2 at the muscular tissue.

This work was partially supported by the Core Research for Evolutional Science and Technology, JST, and Health Science Research Grants (Artificial Blood Project) of the Ministry of Health and Welfare, Japan.

References and Notes

CREST investigator, Japan Science and Technology Corporation
1 M. Momenteau and C. A. Reed, *Chem. Rev.*, **94**, 659 (1994) and references therein.
2 J. P. Collman, J. I. Brauman, K. M. Doxsee, T. R. Halbert, E. Bunnenberg, R. E. Linder, G. N. LaMar, J. D. Gaudio, G. Lange, and K. Spartalian, *J. Am. Chem. Soc.*, **102**, 4182 (1980).
3 A. R. Battersby and A. D. Hamilton, *J. Chem. Soc., Chem. Commun.*, **1980**, 117.
4 J. E. Baldwin, J. H. Cameron, M. J. Crossley, I. J. Dagley, S. R. Hall, and T. Klose, *J. Chem. Soc., Dalton Trans.*, **1984**, 1739.
5 A. Van der Heijden, H. G. Peter, and A. H. A. Van der Oord, *J. Chem. Soc. D*, **1971**, 369.
6 P. K. Warme and L. P. Hager, *Biochemistry*, **9**, 1599; 1606 (1970).
7 M. Momenteau, M. Rougee, and B. Loock, *Eur. J. Biochem.*, **71**, 63 (1976).
8 E. Tsuchida, T. Komatsu, S. Kumamoto, K. Ando, and H. Nishide, *J. Chem. Soc., Perkin Trans 2*, **1995**, 747.
9 Spectroscopic data: **1a**; ^{1}H NMR (500 MHz, $CDCl_3$) δ –2.6 (s, 2H, innerH), 0.0–0.1 (m, 36H, *t*-Bu), 1.9 (t, 2H, –CH_2C(=O)NH–His), 2.3–2.4 (m, 4H, –(CH_2)$_2$C(=O)O–), 3.2 (s, 2H, Im–CH_2–), 3.7 (m, 3H, His–OMe), 4.8 (s, 1H, Im–CH_2C*H*–), 5.3–5.4 (q, 2H, pyrrole-β-CH_2–), 6.8 (s, 1H, Im), 7.4–7.4 (m, 8H, amide-H, phenyl-4), 7.6 (s, 1H, Im), 7.8 (m, 8H, phenyl-3,5), 8.6–8.8 (m, 11H, pyrrole-β–H, phenyl-6). FAB-MS (*m/z*): 1304.8 [M^+–H]. IR (cm^{-1}): 1687 ($\nu_{C=O}$(amide)), 1740 ($\nu_{C=O}$ (ester)). UV–vis ($CHCl_3$) λ_{max}: 421, 516, 547, 590, 646 nm. **1b**; FAB–MS (*m/z*): 1360.6 (M^+–Br). IR (cm^{-1}): 1682 ($\nu_{C=O}$(amide)), 1741 ($\nu_{C=O}$ (ester)). UV–vis ($CHCl_3$) λ_{max}: 353, 420, 507, 577 nm. **2a**; ^{1}H NMR (500 MHz, $CDCl_3$) δ –2.6 (s, 2H, innerH), 0.0–0.1 (m, 12H, 1–Me), 0.3–1.0 (m, 40H, cyclohexyl), 1.9 (t, 2H, –CH_2C(=O)NH–His), 2.3–2.5 (m, 4H, –(CH_2)$_2$C(=O)O–), 3.2 (s, 2H, Im–CH_2–), 3.7 (m, 3H, His–OMe), 4.9 (s, 1H, Im–CH_2C*H*–), 5.2–5.4 (q, 2H, pyrrole-β-CH_2-), 7.1 (s, 1H, Im), 7.4–7.5 (m, 8H, amide-H , phenyl-4), 7.7 (s, 1H, Im), 7.8 (m, 8H, phenyl-3,5), 8.7–8.8 (m, 11H, pyrrole-β–H, phenyl-6). FAB–MS (*m/z*): 1465.8 (M^+–H). IR (cm^{-1}): 1684 ($\nu_{C=O}$(amide)), 1740 ($\nu_{C=O}$ (ester)). UV–vis. ($CHCl_3$) λ_{max}: 423, 517, 549, 591, 646 nm. **2b**; FAB–MS (*m/z*): 1520.8 (M^+–Br). IR (cm^{-1}): 1693 ($\nu_{C=O}$(amide)), 1740 ($\nu_{C=O}$ (ester)). UV–vis ($CHCl_3$) λ_{max}: 354, 420, 505, 581 nm.
10 H. Hori and T. Kitagawa, *J. Am. Chem. Soc.*, **102**, 3608 (1980).
11 J. Wu, T. Komatsu, and E. Tsuchida, *J. Chem. Soc., Dalton Trans.*, **1998**, 2503.
12 J. M. Burke, J. R. Kinchard, S. Peters, R. R. Gagne, J. P. Collman, and T. G. Spiro, *J. Am. Chem. Soc.*, **100**, 6083 (1978).
13 The esff forcefield simulation was performed using an Insight II system (Molecular Simulations Inc.). The structure was generated by alternative minimizations and annealing dynamic calculations from 1000 K to 100 K.
14 J. P. Collman, J. I. Brauman, B. L. Iverson, J. L. Sessler, R. M. Morris, and Q. H. Gibson, *J. Am. Chem. Soc.*, **105**, 3052 (1983).
15 T. G. Traylor, S. Tsuchiya, D. Campbell, M. Mitchell, D. Stynes, and N. Koga, *J. Am. Chem. Soc.*, **107**, 604 (1985).